
Article:
Adeyemi, OO orcid.org/0000-0002-0848-5917, Sherry, L orcid.org/0000-0002-4367-772X, Ward, JC et al. (4 more authors) (2019) Involvement of a Nonstructural Protein in Poliovirus Capsid Assembly. Journal of Virology, 93 (5). e01447-18. ISSN 0022-538X

https://doi.org/10.1128/JVI.01447-18

Involvement of a non-structural protein in poliovirus capsid assembly.

Oluwapelumi O. Adeyemi, Lee Sherry, Joseph C. Ward, Danielle M. Pierce, Morgan R. Herod, David J. Rowlands[#] and Nicola J. Stonehouse[#]

School of Molecular and Cellular Biology, Faculty of Biological Sciences, University of Leeds, Leeds, United Kingdom

Running title: A non-structural protein in PV assembly

Address correspondence to David J. Rowlands, d.j.rowlands@leeds.ac.uk or Nicola J. Stonehouse, N.J.Stonehouse@leeds.ac.uk

Keywords: poliovirus, $2A^{pro}$, cleavage, evolution, selection

Word count

Abstract: 229; Importance: 86; Body text: 5,141

Abstract

Virus capsid proteins must perform a number of roles. These include the ability to self–assemble and to maintain stability under challenging environmental conditions, while retaining the conformational flexibility necessary to uncoat and deliver the viral genome into a host cell. Fulfilling these roles could place conflicting constraints on the innate abilities encoded within the protein sequences. In a previous study, we identified a number of mutations within the capsid coding sequence of poliovirus (PV) that were established in the population during selection for greater thermostability by sequential treatment at progressively higher temperatures. Two mutations in the VP1 protein acquired at an early stage were maintained throughout this selection procedure. One of these mutations prevented virion assembly when introduced into a wild type (wt) infectious clone. Here, we show by sequencing beyond the capsid coding region of the heat selected virions, that two mutations had arisen within the coding region for the 2A protease. Both mutations were maintained throughout the selection process. Introduction of these mutations into a wt infectious clone by site-directed mutagenesis considerably reduced replication. However, they permitted a low level of assembly of infectious virions containing the otherwise lethal mutation in VP1. The $2A^{pro}$ mutations were further shown to slow the kinetics of viral polyprotein processing and we suggest that this delay improves the correct folding of the mutant capsid precursor protein to permit virion assembly.

Importance

RNA viruses including poliovirus evolve rapidly due to the error-prone nature of the polymerase enzymes involved in genome replication. Fixation of advantageous mutations may require the acquisition of complementary mutations which can act in concert to achieve

a favourable phenotype. This study highlights a compensatory role of a non-structural regulatory protein, $2A^{pro}$, for an otherwise lethal mutation of the structural VP1 protein to facilitate increased thermal resistance. Studying how viruses respond to selection pressures is important for understanding mechanisms which underpin emergence of resistance and could be applied to the future development of antiviral agents and vaccines.

48 **Introduction**

49 RNA viruses have high mutation rates that contribute to population diversity, genetic
50 robustness, and ability to withstand population bottlenecks (1, 2). The RNA-dependent RNA
51 polymerase enzyme (RdRp) lacks a proof reading function, thereby resulting in error-prone
52 replication. As a result, RNA viruses exist as swarms of variants, also known as quasispecies.
53 As viruses adapt under altered growth constraints, mutants with replicative advantage in the
54 face of selection emerge from the quasispecies and alter the population sequence
55 composition. However, this may occur at a cost to virus fitness (1, 3).

56 Poliovirus (PV), which occurs as three serotypes, PV 1-3, is a picornavirus with a 7.5 kb
57 positive sense single-stranded RNA genome enclosed within a 30 nm icosahedral capsid. The
58 genome (figure 1A) comprises a coding region, which is flanked at the 5' and 3' ends by
59 untranslated regions (UTR) (4). Upon cell entry the coding region is translated into a
60 polyprotein precursor which is cleaved by viral proteases, $2A^{pro}$ and $3C^{pro}$ (or its precursor
61 $3CD^{pro}$). Upon translation, the structural precursor protein, P1, is autocatalytically cleaved
62 from the polyprotein by $2A^{pro}$ (5) and P1 is further processed into VP1, VP3 and VP0 by
63 $3C^{pro}$/ $3CD^{pro}$. The two non-structural precursors, P2 and P3 are processed into $2A^{pro}$, 2B, 2C
64 and 3A, 3B, $3C^{pro}$, $3D^{pol}$ respectively, again by $3C^{pro}$/ $3CD^{pro}$ (6, 7). Replication of the PV
65 genome is mediated by the RdRp $3D^{pol}$ (8) and primed by 3B within a membrane-bound
66 complex that also includes 2B, 2C (9, 10) and 3A (11) with roles reviewed in (12).

67 The PV $2A^{pro}$ is a cysteine protease that has been described as a multi-functional regulatory
68 protein due to its roles at various stages of the viral lifecycle (reviewed in (13)). It has an
69 active site that comprises a catalytic triad - H20, D38, and C109 (14, 15), as well as highly
70 conserved cysteine and histidine residues C55, C57, C115, and H117 that have been shown to
71 be critical for maintaining structural integrity and for *cis*- and *trans*- catalytic activities (16,

72 17). The PV $2A^{pro}$ has been shown to stimulate IRES-mediated viral translation over cap-
73 dependent translation of host mRNA through inactivation of a key host cellular translation
74 initiation factor, eIF4G (18-20). It has also been shown to have a role in the control of
75 genome replication by stimulating negative-strand RNA synthesis and enhancing RNA
76 stability (21, 22). $2A^{pro}$ also plays a key role in virion assembly (5) by cleaving the P1 region
77 from the polyprotein. This is followed by the self-assembly of VP0, VP3 and VP1 into
78 genome-free capsids or around the nascent genome to form virion particles in which VP0 is
79 cleaved into VP2 and VP4. It has been shown for the attenuated Sabin vaccine strains of PV-
80 2 and PV-3 that $2A^{pro}$ can compensate for cell-specific attenuating mutations within the
81 5'UTR (23). Additionally, a study recently reported on compensatory $2A^{pro}$ mutations within
82 acid-resistant enterovirus D94 variants that evolved capsid-stabilising mutations (24).
83 Together, these findings suggest important roles for $2A^{pro}$ in the evolution of picornaviruses,
84 however, the mechanisms responsible are unclear.

85 We recently described the evolution of heat resistant PV-1 capsids through multiple cycles of
86 thermal selection (25). Here, we characterise mutations within the non-structural protein of
87 the thermally-selected virus populations and describe the mechanism by which these
88 facilitated the correct assembly of the heat resistant capsids.

89 **Results**

90 **Analysis of a population of PV-1 evolving during sequential thermal stressing.**

91 Previously, we employed *in vitro* selection of PV-1 by sequential heating in order to select
92 mutations in the viral structural proteins that increased the thermal stability of the capsid (25).
93 Here, we determined the consensus sequence of the evolving population at each passage
94 during the selection (figure 1B). VP1-V87A was the first capsid mutation observed within the
95 population following three selection cycles at 51°C. After five further cycles of selection at
96 51°C, VP1-I194V also appeared, after which both mutations were maintained in the
97 consensus sequence of all subsequent virus populations selected at 51°C (VS51), 53°C
98 (VS53) and 57°C (VS57) . We introduced each of the capsid protein mutations identified in
99 VS51, VS53 and VS57 (figure 1B) into an infectious clone of PV-1 and showed that I194V
100 alone prevented virus assembly. For these experiments *in vitro* generated T7 RNA transcripts
101 of the mutated genomes were transfected into mouse L-cells and the harvested virions were
102 titrated using HeLa cells (table 1). The use of L-cells (that do not possess the PV receptor)
103 ensured single cycle infection.

104 We extended our sequence analyses beyond P1 and showed that in addition to the capsid
105 mutations identified in VS51, two non-structural mutations were identified within the 2A^{pro}
106 region of the genome (i.e. 2A-I99V and 2A-G102R) and were maintained in further rounds of
107 thermal selection (figure 1B). No other non-synonymous mutations were identified within the
108 populations, however, synonymous mutations were identified in VS53 (i.e. 2A-G95
109 [GGC/GGA], 2A-G101 [GGC/GGG]) and VS57 (i.e. 2C- V47 [GTA/GTG]). The level of
110 conservation of the two substituted 2A^{pro} residues among enterovirus species was
111 investigated through the alignment of 2A^{pro} reference sequences of representative members
112 i.e. enteroviruses A, B, C, D, E, F, G & H and rhinovirus A, B and C. This showed that 2A-

113 I99 is highly conserved among enterovirus C species but varies among other enteroviruses;
114 while 2A-G102 is highly conserved across all enterovirus species (figure 1C). As a
115 multifunctional protein known to play important roles during translation (18-20), replication
116 (21, 22) and morphogenesis (5, 26) of PV, we investigated the significance of the mutations
117 selected in $2A^{pro}$ during adaptation to thermal stress.

118 **Effects of 2A-I99V and 2A-G102R on the *cis* cleavage activity of $2A^{pro}$**

119 The structure of $2A^{pro}$ (27) comprises a catalytic triad (14, 15) and highly conserved cysteine
120 and histidine residues that maintain the catalytic activity and structural integrity of $2A^{pro}$,
121 respectively (16, 28). Neither of the 2A mutations identified here involved these residues,
122 however, proximity to a catalytic residue (C109) could affect activity (13-16, 26). $2A^{pro}$ has
123 been shown to autocatalytically cleave the viral polyprotein *in cis* between tyrosine and N38
124 glycine residues at the P1/2A junction (26, 28-31). To investigate this cleavage by the mutant
125 versions of $2A^{pro}$, non-replicative sub-genomic constructs of the P1 region with 2A (i.e. P1-
126 2A) were cloned into a pcDNA 3.1(+) vector (figure 2A) and termed pcDNA-P1/2A,
127 pcDNA-P1/$2A_{I99V}$, pcDNA-P1-$2A_{G102R}$ and pcDNA-P1/$2A_{I99V/G102R}$. These constructs were
128 expressed using an *in vitro* coupled transcription/translation (T_NT) system under the
129 transcriptional control of a T7 promotor and translated in the presence of ^{35}S (cys/met) for 90
130 minutes at 30ºC. Excess unlabelled cys/met was then added to prevent further ^{35}S
131 incorporation. Samples were harvested at 30-minute intervals to assess *cis*-cleavage of the
132 P1-2A sub-genomic precursor.

133 We confirmed that the wt precursor P1/2A, and also the 2A-I99V construct efficiently self-
134 processed to produce P1 and 2A. However, processing of the 2A-G102R construct was
135 severely restricted when this mutation was present individually or in combination with 2A-
136 I99V (figure 2B). Quantitative analyses of the autoradiographs were undertaken, in

137 comparison with processing of the wt proteins. The data showed that 2A-G102R alone, or in
138 combination with 2A-I99V, reduced the amount of processed P1/2A precursor (figure 2C) by
139 46% and 58%, respectively. The amount of P1 product from 2A-G102R alone or combination
140 with 2A-I99V was similarly reduced by 46% and 58%, respectively over the wt levels (figure
141 2D).

142 **Effects of $2A^{pro}$ mutations (I99V/G102R) on PV-1 polyprotein processing**

143 Since the proteolytic activity of $2A^{pro}$ on the truncated P1-2A polyprotein was affected by the
144 selected $2A^{pro}$ mutations (figure 2), we investigated downstream effects of the $2A^{pro}$
145 mutations on processing of the full length viral polyprotein using a HeLa cell-free system
146 (32, 33). A combination of both $2A^{pro}$ mutations was introduced into cDNA clone
147 pT7RbzPV1 using site-directed mutagenesis (SDM) to create pT7RbzPV1-$2A_{I99V/G102R}$.
148 RNA transcripts of pT7RbzPV1 or pT7RbzPV1-$2A_{I99V/G102R}$ were translated for 2 hours in a
149 HeLa cell-free lysate in the presence of ^{35}S (cys/met). Following a chase with excess
150 unlabelled cys/met, polyprotein processing was assayed by SDS-PAGE and autoradiography
151 as shown in lanes 1-12 of figure 3A. To help identify cleavage products we generated
152 predefined proteins from pcDNA 3.1(+) vectors. Non-cleavable P1-P2 (termed pcDNA-P1-
153 P2) and P1-2A (termed pcDNA-P1-2A) were generated by incorporating the mutation 2A-
154 C109A, which ablates catalytic activity of $2A^{pro}$ (14). Additionally, sub-genomic constructs
155 of P1 only (termed pcDNA-P1) and P2 only (termed pcDNA-P2) were generated. Sub-
156 genomic constructs inserted into pcDNA 3.1(+) vectors were expressed in T_NT assays and
157 incubated at 30°C for 3 hours in the presence of ^{35}S (cys/met). The expressed proteins were
158 used as markers to identify protein band patterns produced by polyprotein processing as
159 shown in lanes 14 – 17 of figure 3A.

160 As shown in lanes 1, 3, 5, 7, 9 and 11 of figure 3A, the processing profile and kinetics for the
161 wt polyprotein followed an expected pattern, with co-translational release of P1 through
162 autocatalytic cleavage by $2A^{pro}$, followed by the processing of P2-P3 and further processing
163 of P2 and P3 (6, 26). In contrast, the reduced autocatalytic processing of the polyprotein
164 produced from the mutant construct pT7RbzPV1-$2A_{I99V/G102R}$ resulted in delayed appearance
165 of several intermediate products and two large sub-genomic precursor proteins (lanes 2, 4, 6,
166 8, 10 and 12) of similar sizes to uncleaved P1-P2 (lane 14) and P1-2A (lane 15) were
167 detected. To determine processing rates, band intensities were analysed using ImageJ. A
168 precursor corresponding to P1-P2, which was seen in mutant 2A-I99V/G102R but not in wt,
169 was slowly processed over 24 hours (figure 3B). A precursor corresponding to P1-2A, which
170 could be detected in wt but was more evident in mutant 2A-I99V/G102R, was processed
171 slower in the latter (figure 3C). This suggested that $3CD^{pro}$/$3C^{pro}$ processing of these
172 precursors was less efficient in the mutant 2A-I99V/G102R.

173 **Effects of $2A^{pro}$ mutations (I99V/G102R) on genome replication**

174 It has been reported that although $2A^{pro}$ has no direct effect on positive-strand RNA
175 synthesis, it has a stimulatory role on negative strand synthesis and thereby could regulate
176 RNA replication (21). We therefore investigated the effects of the $2A^{pro}$ mutations on viral
177 replication using a modified version of cDNA clone pT7RbzPV-1. Here, the P1 capsid
178 precursor was replaced with the green fluorescent protein (GFP) coding sequence from
179 *Ptilosarcus gurneyi*, creating a sub-genomic replicating replicon, termed pRepPV1 (figure
180 4A). Both $2A^{pro}$ mutations were introduced into pRepPV1 individually (to create pRepPV1-
181 $2A_{I99V}$, pRepPV1-$2A_{G102R}$) or in combination (to create pRepPV1-$2A_{I99V/G102R}$). A
182 replication-deficient construct with a double point mutation (GDD to GNN) in the $3D^{pol}$
183 active site (34) was used as a control for input translation. *In vitro* transcribed RNAs were

184 generated from the replicon constructs and transfected into HeLa cells. Replication kinetics
185 were monitored in real time using an IncuCyte Zoom system as described in the methods
186 section. The data are shown in Figure 4A, with end-point data shown in Figure 4B for clarity.
187 The 2A-I99V replicon replicated at levels similar to wt, however, replication of the 2A-
188 G102R or 2A-I99V/G102R replicons was approximately 100-fold lower than wt ($p<0.0001$),
189 although still 10-fold higher than the input translation levels of the replication-deficient GNN
190 replicon ($P<0.05$). Rate of replication of 2A-I99V was similar to wt but there was a lag for
191 2A-G102R and 2A-I99V/G102R. This shows that the presence of the 2A-G102R mutation
192 resulted in a significant reduction in RNA replication.

193 **The $2A^{pro}$ mutations can rescue assembly-defective capsid mutations.**

194 In our previous report, we showed that populations of PV-1 thermally-selected at 51°C
195 possessed two common VP1 mutations (i.e. I194V and V87A) (25), both of which were
196 maintained through further selection cycles. We introduced both mutations individually into
197 pT7Rbz-PV1 and showed that V87A was compatible with the production of infectious
198 virions but the construct with VP1-I194V could not assemble infectious particles (25). Since
199 both $2A^{pro}$ mutations were propagated alongside the VP1 mutations during selection (figure
200 1B), we investigated here whether the $2A^{pro}$ mutations could rescue the assembly-deficient
201 phenotype of the VP1-I194V mutant.

202 Infectious clones of PV-1 (pT7Rbz-PV1) with the $2A^{pro}$ mutations I99V/G102R (pT7Rbz-
203 PV1-$2A_{I99V/G102R}$) or the assembly-deficient mutation VP1-I194V alone (i.e. pT7Rbz-PV1-
204 $VP1_{I194V}$) or in combination with the $2A^{pro}$ mutations (i.e. pT7Rbz-$PV1_{I194V}$-$2A_{I99V/G102R}$)
205 were generated. T7 RNA transcripts of all four constructs were transfected into HeLa cells or
206 mouse L-cells. After 24 hours incubation at 37°C virus particles were harvested by freeze-
207 thawing cells and clarification of the supernatants. Titres of infectious virions harvested from

208 both transfected cell lines were determined by plaque assays using HeLa cells, while thermal
209 stabilities of the recovered virions were assessed as previously described (25).

210 The PV-1 titres from L-cells and HeLa cells transfected with the mutant construct containing
211 the 2A-I99V/G102R were reduced by 5 $\log_{10}$ PFU/ml (figure 5A) and 3 $\log_{10}$ PFU/ml (figure
212 5B), respectively. In the L-cells, VP1-I194V alone did not produce infectious virions, as
213 expected. It should be noted that L-cells lack the PV receptor and therefore only support
214 single-cycle infection. Therefore, virions produced in HeLa cells were possible revertants
215 amplified through cell to cell spread. Our data further showed that VP1-I194V in
216 combination with 2A-I99V/G102R resulted in infectious virion titres in both L-cells and
217 HeLa cells similar to those of infectious clones with wt P1 and both 2A mutations.
218 Furthermore, the thermal inactivation profile of the recovered virus showed that VP1-I194V-
219 2A-I99V/G102R was more thermally stable than wt or 2A-I99V/G102R (figure 5C).
220 Together, these data suggest that the mutation VP1-I194V provided thermal stability to the
221 viral capsid as expected (25) and that the 2A mutations allowed rescue of this mutant.

222 To assess genetic stability of the population, virus mutant VP1-I194V-2A-I99V/G102R was
223 passaged in the absence of selection pressure using HeLa cells until viral titres were
224 equivalent to wt. Sequencing of these 'restored' virions showed that the $2A^{pro}$ second site
225 (compensatory) mutations had reverted in the absence of selection pressure (data not shown) .

226 **$2A^{pro}$ mutations do not act by reducing translation.**

227 Assembly of icosahedral viral capsids is a complex process which is not yet fully understood.
228 A study with the plant virus, brome mosaic virus, suggested that slower translation of the
229 capsid proteins could result in enhanced assembly (35). In view of these observations we
230 investigated the consequences of reducing translation efficiency of the PV-1 infectious clone
231 incorporating the VP1-I194V mutation on the recovery of virions.

232 Cycloheximide is known to inhibit eukaryotic protein synthesis by stopping ribosomal
233 elongation during translation (36) and micromolar concentrations of cycloheximide have
234 been shown to shut off PV-1 translation in HeLa cells (37, 38). To determine whether partial
235 inhibition of translation could replicate the assembly compensatory effects of the $2A^{pro}$
236 mutations we investigated the effect of reducing/slowing translation of PV-1 in L-cells using
237 low concentrations of cycloheximide. First, we used conventional cytotoxicity assays to
238 demonstrate an IC_{50} of 420 nM in mouse L cells (figure 6A). To determine concentrations at
239 which PV-translation can be reduced but not eliminated, transfected mouse L-cells were
240 treated with increasing concentrations of cycloheximide at 1.5 hours post-transfection and
241 incubated at 37°C for 24 hours. Cell lysates and supernatants were harvested and
242 immunoblotted for viral capsid protein (VP1).

243 As expected, detection of VP1 decreased as concentrations of cycloheximide increased
244 (figure 6B). We therefore investigated recovery of assembly-deficient VP1-I194V mutant by
245 treating transfected L-cells with sub-lethal concentrations of cycloheximide at 1.5 hours post-
246 transfection. Cells were lysed, clarified and infectious titres of supernatant samples were
247 determined by plaque assays. Our data show that treatment with cycloheximide could not
248 recover the assembly-deficient VP1-I194V mutant (figure 6C). Therefore it appears that
249 recovery of the assembly deficient VP1-I194V mutant by $2A^{pro}$ cannot be replicated by
250 partial pharmacological inhibition of protein translation.

251 **Discussion**

252 Virions must be sufficiently stable to protect their genome from environmental damage but
253 flexible enough to allow the conformational changes required to deliver the genome into a
254 new host cell (7, 39). It is likely that changes to this balance, which might occur during
255 adaptation to unusual environmental stress, will be acquired at a cost to overall fitness (1, 3).

256 Previously, we reported the thermal selection of PV-1 at increasing temperatures of 51°C,
257 53°C and 57°C which resulted in virus populations that consistently maintained two VP1
258 mutations (i.e. I194V and V87A). We further showed by site-directed mutagenesis of a wt
259 infectious clone that a combination of VP1-I194V and VP1-V87A increased the thermal
260 stability of the PV-1 capsid while VP1-I194V alone abrogated virion production (25). It has
261 been shown that VP1-I194 in all PV serotypes (or the equivalent VP1-I192 in PV-3) plays an
262 important role in acquiring resistance to a pocket-binding antiviral compound V-073 (40, 41).
263 Additionally, VP1-V87A has been reported to confer heat resistance to PV-1 (42).
264 Previously, we showed that the selected population containing both VP1 mutations (I194V
265 and V87A) was more thermally stable than the wt infectious clone (25). Our findings
266 suggested that VP1-I194V evolved to complement VP1-V87A, at a cost to fitness. This was,
267 however, partially compensated for by two non-structural protein mutations within the $2A^{pro}$
268 region of the genome (2A-I99V and 2A-G102R). We found that both sets of VP1 heat-
269 resistance and $2A^{pro}$ mutations were maintained together as consensus during further rounds
270 of selection (figure 1B and 1C), suggesting their importance in maintaining the thermostable
271 phenotype. Here, we sought to understand the functional and biological consequences of the
272 $2A^{pro}$ mutations during adaptation.

273 Multiple roles for $2A^{pro}$ have been reported, which include antagonising host immune
274 responses (13), prolonging viral RNA translation (18, 19), stabilising replicating RNA (22),
275 enhancing RNA synthesis (21) and initiating morphogenesis (5). Thus, $2A^{pro}$ has been
276 suggested to play a regulatory role in the PV lifecycle (13). The autocatalytic *cis*-cleavage
277 activity of $2A^{pro}$ occurs co-translationally with high efficiency (figure 2B), while further
278 polyprotein processing by $3C^{pro}$ occurs much less efficiently (26). The proteolytic activity of
279 $2A^{pro}$ can be affected by mutations in the catalytic triad (14, 15) or via highly conserved
280 cysteine and histidine resides known to maintain structural integrity (16, 27). Although the

281 selected $2A^{pro}$ mutations did not involve any of these residues, we hypothesised that
282 proximity of 2A-G102R to a catalytic residue (i.e. C109) could affect catalytic activity.

283 The co-translational cleavage of P1/2A occurs rapidly during normal virus replication. This
284 appeared to be slower in the rabbit reticulocyte T_NT assays used here, which have also been
285 reported to restrict *in vitro* translation of poliovirus RNA (43). However, it provides a useful
286 platform to investigate post-translational cleavage kinetics of PV. Using the T_NT assay to
287 investigate the proteolytic efficiency of the selected $2A^{pro}$ mutations, we observed that 2A-
288 I99V had no effect on the *cis* cleavage of the predefined P1-2A construct, however, 2A-
289 G102R individually and in combination with 2A-I99V slowed the *cis* cleavage of P1-2A. We
290 therefore hypothesised that the slower processing could have resulted in downstream effects
291 on other aspects of the viral lifecycle such as delayed release of P1 and 2BC which could
292 influence capsid assembly and/or genome replication.

293 Using the HeLa cell-free system we were able to investigate the *cis*-cleavage of the entire
294 polyprotein by the mutant $2A^{pro}$. This showed an accumulation of large precursors, P1-P2 and
295 P1-2A, with an abundance of the former. Both of these precursor proteins were slowly
296 processed by the protease $3C/3CD^{pro}$. The replication of PV has been shown to involve the
297 formation of a membrane-bound complex of 2B, 2C (9, 10) and 3A (11). We speculate that
298 the delayed release of 2BC may have resulted in delayed recruitment of 2B and 2C to this
299 replication complex (9, 10) and thus genome replication was significantly affected (figure 4).
300 Given the global change to the order in which the precursor protein is cleaved it is perhaps
301 surprising that virus replication is still supported. Such global changes to how polyproteins
302 are processed could provide a mechanism by which positive-sense RNA viruses can quickly
303 adapt to selection pressures via changing the repertoire and order of proteins produced
304 through protease mutations.

305 Although we do not fully understand the role of 2A-I99V, the maintenance of this mutation
306 together with G102R within the consensus sequence, prompted our investigation of the
307 combined effects of both mutations on the VP1-I194V capsid mutant. Our results suggested
308 that the 2A mutations compensated for the assembly-deficient VP1-I194V mutant (25)
309 (figure 5). Together, our data suggest that a combination of 2A-I99V and 2A-G102R
310 modulated the *cis*-mediated cleavage of P1 (9, 10)and significantly decreased the rates of
311 genome replication to alter the dynamics of virion assembly and overcome the otherwise
312 deleterious effect of VP1-I194V capsid mutation. (44)However, further investigation will be
313 required to fully understand the mechanisms through which the $2A^{pro}$ mutations affected
314 replication of the genome.

315 Assembly of the PV capsid is a complex process requiring highly efficient translation, which
316 can be lethally affected by de-optimisation of the capsid codons (45). In our previous study
317 we reported that thermal selection of PV-1 (generating variants with thermally stable capsids)
318 occurred at a cost to virion assembly which was due to a VP1-I194V mutation. We further
319 speculated that a capsid-stabilising mutation, VP1-V87A, could ameliorate the assembly-
320 deficiency effects of VP1-I194V through unknown mechanisms (25). Here, we have traced
321 the selection of VP1-I194V to the coexistence of a pair of second site (compensatory)
322 mutations within $2A^{pro}$, which may have sustained VP1-I194V within the quasispecies. The
323 role of V87A is unclear but the coexistence of I194V and V87A in all subsequently selected
324 heat resistant viruses suggests a functional link between these two mutations. Our findings
325 also showed that partial inhibition of translation of the polyprotein using cycloheximide could
326 not recover the assembly-deficient VP1-I194V mutant (figure 6), however, reduction of the
327 rate of polyprotein processing by the mutations (2A-I99V and 2A-G102R) appeared to favour
328 assembly. Together our findings suggest that recovery of the assembly deficient VP1-I194V
329 mutant by $2A^{pro}$ may have involved a chaperone-like activity provided by $2A^{pro}$.

330 Chaperones prevent aggregation of proteins in highly crowed cellular environments (30, 31),
331 and facilitate viral capsid assembly. Host-encoded chaperones have been reported for
332 enteroviruses including PV (46), hepatitis B virus (47), bacteriophages (48, 49). While some
333 virally-encoded proteins have been reported to have chaperone-like activities that facilitate
334 capsid assembly in some viruses e.g. the capsid-associated protein 80 (p80) of African swine
335 fever virus (50), T-antigen (TAg) of SV40 (51) and the non-structural protein 40 (NSP40) of
336 herpes simplex virus (52). Early stage morphogenesis of PV is facilitated by the host-encoded
337 chaperone, Hsp70 (46) while virally-encoded 2C facilitates later stages of morphogenesis of
338 virions (i.e. genome encapsidation) (12, 53-55).

339 Owing to their small genome sizes, virus encoded proteins such as $2A^{pro}$ have been shown to
340 perform multiple roles. Our study provides the first suggestion that PV $2A^{pro}$ could act as a
341 chaperone-like protein and suggests (14, 32, 56) regulatory roles for $2A^{pro}$ in maintaining the
342 balance between virus fitness and virion stability that allows the emergence of heat-resistant
343 PV-1 variants.

344 **Methods**

345 **Antibodies**

346 Rabbit polyclonal anti-GAPDH (G9545) and anti-Rabbit polyclonal (A0545) antibodies were
347 commercially sourced from Sigma-Aldrich (now Merck), Germany. Mouse monoclonal anti-
348 poliovirus 1 (VP1) antibody, MAB8560 was commercially sourced from Millipore (now
349 Merck), Germany.

350 **Cell lines and virus propagation**

351 HeLa and mouse L-cells were obtained from the National Institute of Biological Standards
352 and Control, UK. Viruses were propagated by standard methods. Infectivity titres were
353 determined by plaque assays using HeLa monolayer cells (57) and expressed as plaque
354 forming units per millilitre (PFU/ml).

355 **Viral genome extraction and sequencing**

356 RNA was extracted from virion samples using guanidinium thiocyanate-phenol-chloroform,
357 (58). The sequence from the 5' UTR to the end of the structural (P1) coding region (i.e.
358 nucleotide positions 1 to 3,385 within the genome) was reverse transcribed and PCR-
359 amplified using previously-described downstream (P1Rev) and upstream (P1Fwd) primers
360 5'-CTTGGCCACTCAGGATGATT-3' and 5'-TTAAAACAGCTCTGGGGTTGTAC-3',
361 respectively (25). Both structural and non-structural regions (i.e. nucleotide positions 1 to
362 7,407 within the genome) were reverse transcribed and PCR-amplified using downstream
363 (P3Rvs) and upstream (P1Fwd) primers 5'-GTATGACCCAATCCAATTCGACT-3' and 5'-
364 TTAAAACAGCTCTGGGGTTGTAC-3', respectively. PCR amplicons were sequenced by
365 Sanger methods (59) and cloned into pGEMT-easy vector and individual colonies sequenced
366 (60). Primer sequences are available on request.

367 **Recombinant DNA techniques**

368 Poliovirus was recovered from an infectious clone sourced from Bert Semler, University of
369 California. The full PV-1 (Mahoney) genome was cloned into vector pT7Rbz that
370 incorporates a T7 RNA polymerase promoter to allow *in vitro* RNA synthesis, and a
371 ribozyme overhang (61). For the *in vitro* assay, the PV-1 P1/2A precursor was cloned into
372 vector pcDNA 3.1(+) with a Kozak sequence. Several sub-genomic constructs were designed
373 and incorporated into a pcDNA 3.1(+) vector. These included pcDNA-P1-2A (which has a wt
374 P1-2A), pcDNA-P1-2A$_{I99V}$ (which has a wt P1 and I99V mutation introduced to 2A),
375 pcDNA-P1-2A$_{G102R}$ (which has a wt P1 and G102R mutation introduced to 2A), pcDNA-P1-
376 2A$_{I99V/G102R}$ (which has a wt P1 and a combination of I99V and G102R mutation introduced
377 to 2A), pcDNA-P1-P2 (i.e. a non-cleavable P1-P2 construct with a 2A-C109A mutation
378 introduced), pcDNA-P1-2A (i.e. a non-cleavable P1-P2 construct with a 2A-C109A mutation
379 introduced). All mutations were introduced by SDM (62).

380 **Real-time sub-genomic replicon replication assay**

381 Using a previously described PV-1 (strain Mahoney) cDNA clone (pT7RbzPV-1) (25) a sub-
382 genomic replicon was designed and termed pRepPV1-wt. Here, the P1 capsid precursor was
383 replaced with the green fluorescent protein (GFP) coding sequence from *Ptilosarcus gurneyi.*
384 The modified pT7RbzGFP replicon encoded the PV-1: 5'UTR, residues 1-23 of VP0,
385 pTGFP, the last 25 residues of VP3, the PV P2 region, P3 region and the 3'UTR, followed by
386 the rest of pT7Rbz. Both 2A^{pro} mutations were introduced into pRepPV1 individually (to
387 create pRepPV1-2A$_{I99V}$, pRepPV1-2A$_{G102R}$) or in combination (to create pRepPV1-
388 2A$_{I99V/G102R}$) by SDM (62). pRepPV1 was linearized using *EcoR*I and RNA transcribed *in*
389 *vitro* by T7 RNA polymerase (63). A total of 1 µg aliquots of RNA transcripts were
390 transfected into HeLa cells using Lipofectin. Replicon replication was assessed in real time as

391 GFP expression by live cell imaging within the IncuCyte Dual colour zoom which is an
392 automated phase-contrast and fluorescent microscope within a 37°C humidifying CO_2
393 incubator. Cells were monitored every 30 minutes post-transfection for up to 24 hours. Nine
394 images per well were taken at each time to measure the GFP object counts per well, as well
395 as the total fluorescence intensity per well using an integrated software and analysed
396 according to standard methods (64).

397 ***In vitro* transcription/translation assay – rabbit reticulocytes lysates**

398 Sub-genomic PV-1 constructs were cloned into pcDNA 3.1(+) vector individually (i.e.
399 pcDNA-P1-2A, pcDNA-P1-2A$_{I99V}$, pcDNA-P1-2A$_{G102R}$) or in combination (i.e. pcDNA-P1-
400 2A$_{I99V/G102R}$) and expressed in the T_NT Quick Coupled Transcription/Translation System
401 (Promega) in the presence of (^{35}S) cys/met according to manufacturer's protocol. Following
402 an incubation period of 90 minutes at 30ºC, further incorporation of ^{35}S prevented by addition
403 of excess unlabelled cys/ met and samples were taken at intervals of 30 minutes. Proteins
404 were separated by SDS-PAGE (65) and detected by autoradiography (66) and phosphor
405 imaging (67).

406 ***In vitro* transcription/translation assay – HeLa cell-free extracts**

407 HeLa cell (S10) extracts and initiation factor (IF) fractions were gifted by David Barton,
408 University of Colorado, and also prepared according to standard protocols (33, 68). Reaction
409 mixtures contained 50% (v/v) S10, 20% (v/v) IF, 10% (v/v) 10x reaction buffer (10 mM
410 ATP, 2.5 mM GTP, 2.5 mM CTP, 2.5 mM UTP, 600 mM KCH_3CO_2, 300 mM creatine
411 phosphate, 4 mg/ml creatine kinase, and 155 mM HEPES-KOH [pH 7.4]), 3.2µg T7 RNA
412 transcripts and 38 µCi ^{35}S (cys/met). Reactions were incubated at 34˚C for 2 hours and
413 chased with excess amounts of unlabelled cys/ met. Sample proteins were separated by 8%

414 SDS-PAGE, ^{35}S cys/met-labelled proteins were detected by standard protocols of
415 autoradiography (66) and phosphor imaging (67).

416 **Virus recovery from infectious clones**

417 A total of 2.5 x 10^6 mouse L-cells or HeLa cells were transfected with 5 µg of RNA
418 transcripts using Lipofectin according to manufacturer's protocols. Transfected cells were
419 incubated at 37°C for 16 hours and cell harvests titrated for infectivity after disrupting by
420 freeze-thawing.

421 **Cycloheximide cytotoxicity assay**

422 The compound, 4-(2-hydroxyethyl) piperidine-2,6-dione, also known as cycloheximide was
423 commercially sourced from Sigma-Aldrich (now Merck), Germany.

424 Cell culture 96-well vessels were seeded to 4 x 10^4 cells per well. Triplicate wells of seeded
425 cells were treated with cycloheximide at increasing concentrations from picomolar range
426 through nanomolar to micromolar concentrations. Treated and non-treated cells were
427 incubated at 37°C under 5% CO_2 for 24 hours and assayed for toxicity using the 3-(4,5-
428 dimethylthiazol-2-yl)-5-(3-carboxymethoxyphenyl)-2-(4-sulfophenyl)-2H-tetrazolium (MTS)
429 assay kit, Promega CellTiter 96® Aqueous One Solution Cell Proliferation, according to
430 manufacturers' protocol.

431 **Translation inhibition assays**

432 Mouse L-cells were transfected with 3 µg T7 RNA transcripts of a PV-1 infectious clone,
433 pT7Rbz. At 1.5 hours post-transfection, cycloheximide was added to concentrations
434 indicated. Cells were incubated at 37°C under 5% CO_2 and harvested after 24 hours.
435 Supernatants from each well were clarified by centrifugation at 4,000 rpm for 2 minutes.
436 Cells were trypsinised, washed and lysed using radio-immunoprecipitation assay (RIPA)

437 buffer (50 mM Tris-Cl pH 7.4, 150 mM NaCl, 1% NP-40, 0.5% sodium deoxycholate, 0.1%
438 SDS). Proteins were separated by 8% SDS-PAGE (65) and immunoblotted using anti-VP1
439 MAb (69) by standard protocols.**Densitometry**

440 Scanned images were analysed by ImageJ (70) version 1.47t according to standard
441 procedures. Briefly, scanned image blots or phosphor-screened autoradiographs were saved
442 in the Tagged Image File Format (TIFF). Selected bands of interest were individually
443 selected and pixilated band intensities were quantified according to software algorithms.

444 **Genome sequences and alignment**

445 Reference genome sequences of the following viruses were sourced from GenBank and
446 downloaded in the FASTA format: CVA-1 (AGI61097.1), EV1 (AAC63944.2); PV-1
447 (P03300), PV-2 (AAA46912.1), PV-3 (AAN85444.1), CVA-2 (ANQ47259.1), EV-94 (A-
448 BL61316.1), BEV-1 (P12915.3), BEV-2 (ADU34211.1), EV-G1 (AIA21703.1), SV4
449 (AAL69631.2), HRVA (CAA26181.1), HRV-B (ACK37380.1) and HRV-C (ABK29455.2).
450 Alignment of sequences was carried out at the protein level using the MUltiple Sequence
451 Comparison by Log-Expectation (MUSCLE) algorithm of CLC Sequence Viewer Version
452 7.8.1 software.

453 **Statistical analysis**

454 Statistical analysis of mutants against wt was analysed by student t-tests using GraphPad
455 Prism version 7.01 for Windows (GraphPad Software, La Jolla CA).

Acknowledgments

The authors wish to thank past and current members of the Stonehouse/Rowlands group at the University of Leeds for insightful contributions, in particular Jorge Mancilla, Michalis Christoforou, Clare Nicol, Natalie Kingston and Keith Grehan. The authors also wish to thank David Barton (University of Colorado, USA) for HeLa cell extracts and Bert Semler (University of California, USA) for the cDNA of wt PV-1 (strain Mahoney).

Funding

OOA was funded for part of this study by the Tertiary Institution Trust fund (TETfund), Nigeria.

467 **References**

468 1. Fares MA. 2015. Survival and innovation: The role of mutational robustness in evolution.
469 Biochimie 119:254-61.
470 2. Lauring AS, Frydman J, Andino R. 2013. The role of mutational robustness in RNA virus
471 evolution. Nat Rev Microbiol 11:327-36.
472 3. Crotty S, Andino R. 2002. Implications of high RNA virus mutation rates: lethal mutagenesis
473 and the antiviral drug ribavirin. Microbes Infect 4:1301-7.
474 4. Nomoto A, Omata T, Toyoda H, Kuge S, Horie H, Kataoka Y, Genba Y, Nakano Y, Imura N.
475 1982. Complete nucleotide sequence of the attenuated poliovirus Sabin 1 strain genome.
476 Proc Natl Acad Sci U S A 79:5793-7.
477 5. König H, Rosenwirth B. 1988. Purification and partial characterization of poliovirus protease
478 2A by means of a functional assay. Journal of virology 62:1243-1250.
479 6. Tuthill TJ, Groppelli E, Hogle JM, Rowlands DJ. 2010. Picornaviruses. Curr Top Microbiol
480 Immunol 343:43-89.
481 7. Jiang P, Liu Y, Ma HC, Paul AV, Wimmer E. 2014. Picornavirus morphogenesis. Microbiol Mol
482 Biol Rev 78:418-37.
483 8. Van Dyke TA, Flanegan JB. 1980. Identification of poliovirus polypeptide P63 as a soluble
484 RNA-dependent RNA polymerase. Journal of Virology 35:732-740.
485 9. Bienz K, Egger D, Pasamontes L. 1987. Association of Polioviral Proteins of the P2-Genomic
486 Region with the Viral Replication Complex and Virus-Induced Membrane Synthesis as
487 Visualized by Electron-Microscopic Immunocytochemistry and Autoradiography. Virology
488 160:220-226.
489 10. Bienz K, Egger D, Troxler M, Pasamontes L. 1990. Structural Organization of Poliovirus Rna
490 Replication Is Mediated by Viral-Proteins of the P2 Genomic Region. Journal of Virology
491 64:1156-1163.
492 11. Teterina NL, Pinto Y, Weaver JD, Jensen KS, Ehrenfeld E. 2011. Analysis of poliovirus protein
493 3A interactions with viral and cellular proteins in infected cells. J Virol 85:4284-96.
494 12. Richards OC, Ehrenfeld E. 1990. Poliovirus RNA replication. Curr Top Microbiol Immunol
495 161:89-119.
496 13. Castello A, Alvarez E, Carrasco L. 2011. The multifaceted poliovirus 2A protease: regulation
497 of gene expression by picornavirus proteases. J Biomed Biotechnol 2011:369648.
498 14. Hellen CU, Facke M, Krausslich HG, Lee CK, Wimmer E. 1991. Characterization of poliovirus
499 2A proteinase by mutational analysis: residues required for autocatalytic activity are
500 essential for induction of cleavage of eukaryotic initiation factor 4F polypeptide p220. J Virol
501 65:4226-31.
502 15. Yu SF, Lloyd RE. 1991. Identification of essential amino acid residues in the functional activity
503 of poliovirus 2A protease. Virology 182:615-25.
504 16. Yu SF, Lloyd RE. 1992. Characterization of the roles of conserved cysteine and histidine
505 residues in poliovirus 2A protease. Virology 186:725-35.
506 17. Ryan MD, Flint M. 1997. Virus-encoded proteinases of the picornavirus super-group. Journal
507 of General Virology 78:699-723.
508 18. Kräusslich HG, Nicklin MJ, Toyoda H, Etchison D, Wimmer E. 1987. Poliovirus proteinase 2A
509 induces cleavage of eucaryotic initiation factor 4F polypeptide p220. Journal of Virology
510 61:2711-2718.
511 19. Helentjaris T, Ehrenfeld E. 1978. Control of protein synthesis in extracts from poliovirus-
512 infected cells. I. mRNA discrimination by crude initiation factors. Journal of Virology 26:510-
513 521.
514 20. Agol VI, Gmyl AP. 2010. Viral security proteins: counteracting host defences. Nature Reviews
515 Microbiology 8:867.

516 21. Jurgens CK, Barton DJ, Sharma N, Morasco BJ, Ogram SA, Flanegan JB. 2006. 2Apro is a
517 multifunctional protein that regulates the stability, translation and replication of poliovirus
518 RNA. Virology 345:346-57.
519 22. Ehrenfeld E, Brown D. 1981. Stability of poliovirus RNA in cell-free translation systems
520 utilizing two initiation sites. Journal of Biological Chemistry 256:2656-2661.
521 23. Rowe A, Ferguson GL, Minor PD, Macadam AJ. 2000. Coding changes in the poliovirus
522 protease 2A compensate for 5'NCR domain V disruptions in a cell-specific manner. Virology
523 269:284-93.
524 24. Royston L, Essaidi-Laziosi M, Perez-Rodriguez FJ, Piuz I, Geiser J, Krause KH, Huang S,
525 Constant S, Kaiser L, Garcin D, Tapparel C. 2018. Viral chimeras decrypt the role of
526 enterovirus capsid proteins in viral tropism, acid sensitivity and optimal growth
527 temperature. PLoS Pathog 14:e1006962-82.
528 25. Adeyemi OO, Nicol C, Stonehouse NJ, Rowlands DJ. 2017. Increasing Type 1 Poliovirus Capsid
529 Stability by Thermal Selection. J Virol 91:e01586-16.
530 26. Alvey JC, Wyckoff EE, Yu SF, Lloyd R, Ehrenfeld E. 1991. cis- and trans-cleavage activities of
531 poliovirus 2A protease expressed in Escherichia coli. J Virol 65:6077-83.
532 27. Petersen JF, Cherney MM, Liebig HD, Skern T, Kuechler E, James MN. 1999. The structure of
533 the 2A proteinase from a common cold virus: a proteinase responsible for the shut-off of
534 host-cell protein synthesis. The EMBO journal 18:5463-5475.
535 28. Neubauer D, Aumayr M, Gösler I, Skern T. 2013. Specificity of human rhinovirus 2A(pro) is
536 determined by combined spatial properties of four cleavage site residues. The Journal of
537 general virology 94:1535-1546.
538 29. Skern T, Sommergruber W, Auer H, Volkmann P, Zorn M, Liebig H-D, Fessl F, Blaas D,
539 Kuechler E. 1991. Substrate requirements of a human rhinoviral 2A proteinase. Virology
540 181:46-54.
541 30. Gershenson A, Gierasch LM. 2011. Protein folding in the cell: challenges and progress.
542 Current Opinion in Structural Biology 21:32-41.
543 31. Ellis RJ, Hartl FU. 1999. Principles of protein folding in the cellular environment. Current
544 Opinion in Structural Biology 9:102-110.
545 32. Molla A, Paul AV, Wimmer E. 1991. Cell-free, de novo synthesis of poliovirus. Science
546 254:1647-1651.
547 33. Barton DJ, Flanegan JB. 1993. Coupled translation and replication of poliovirus RNA in vitro:
548 synthesis of functional 3D polymerase and infectious virus. J Virol 67:822-31.
549 34. Jablonski SA, Morrow CD. 1995. Mutation of the aspartic acid residues of the GDD sequence
550 motif of poliovirus RNA-dependent RNA polymerase results in enzymes with altered metal
551 ion requirements for activity. Journal of Virology 69:1532-1539.
552 35. Chen C, Kao CC, Dragnea B. 2008. Self-assembly of brome mosaic virus capsids: insights from
553 shorter time-scale experiments. The journal of physical chemistry A 112:9405-9412.
554 36. Schneider-Poetsch T, Ju J, Eyler DE, Dang Y, Bhat S, Merrick WC, Green R, Shen B, Liu JO.
555 2010. Inhibition of eukaryotic translation elongation by cycloheximide and lactimidomycin.
556 Nature chemical biology 6:209-217.
557 37. Barton DJ, Morasco BJ, Flanegan JB. 1999. Translating Ribosomes Inhibit Poliovirus Negative-
558 Strand RNA Synthesis. Journal of Virology 73:10104-10112.
559 38. Gamarnik AV, Andino R. 1998. Switch from translation to RNA replication in a positive-
560 stranded RNA virus. Genes & development 12:2293-2304.
561 39. Brandenburg B, Lee LY, Lakadamyali M, Rust MJ, Zhuang X, Hogle JM. 2007. Imaging
562 poliovirus entry in live cells. PLoS Biol 5:e183-95.
563 40. Ahmad Salarian A, Jalali A, Zare Mirakabadi A, Vatanpour H, F HS. 2012. Cytotoxic Effects of
564 two Iranian Scorpions Odontobuthusdoriae and Bothutus saulcyi on Five Human Cultured
565 Cell lines and Fractions of Toxic Venom. Iran J Pharm Res 11:357-67.

566 41. Kouiavskaia DV, Dragunsky EM, Liu HM, Oberste MS, Collett MS, Chumakov KM. 2011.
567 Immunological and pathogenic properties of poliovirus variants selected for resistance to
568 antiviral drug V-073. Antivir Ther 16:999-1004.
569 42. Shiomi H, Urasawa T, Urasawa S, Kobayashi N, Abe S, Taniguchi K. 2004. Isolation and
570 characterisation of poliovirus mutants resistant to heating at 50°c for 30 min. Journal of
571 Medical Virology 74:484-491.
572 43. Dorner AJ, Semler BL, Jackson RJ, Hanecak R, Duprey E, Wimmer E. 1984. In vitro translation
573 of poliovirus RNA: utilization of internal initiation sites in reticulocyte lysate. Journal of
574 virology 50:507-514.
575 44. Teterina NL, Levenson EA, Ehrenfeld E. 2010. Viable polioviruses that encode 2A proteins
576 with fluorescent protein tags. J Virol 84:1477-88.
577 45. Mueller JE, Bessaud M, Huang QS, Martinez LC, Barril PA, Morel V, Balanant J, Bocacao J,
578 Hewitt J, Gessner BD, Delpeyroux F, Nates SV. 2009. Environmental poliovirus surveillance
579 during oral poliovirus vaccine and inactivated poliovirus vaccine use in Cordoba Province,
580 Argentina. Appl Environ Microbiol 75:1395-401.
581 46. Macejak DG, Sarnow P. 1992. Association of heat shock protein 70 with enterovirus capsid
582 precursor P1 in infected human cells. Journal of Virology 66:1520-1527.
583 47. Lingappa JR, Martin RL, Wong ML, Ganem D, Welch WJ, Lingappa VR. 1994. A eukaryotic
584 cytosolic chaperonin is associated with a high molecular weight intermediate in the
585 assembly of hepatitis B virus capsid, a multimeric particle. The Journal of cell biology 125:99-
586 111.
587 48. Georgopoulos CP, Hendrix RW, Casjens SR, Kaiser AD. 1973. Host participation in
588 bacteriophage lambda head assembly. Journal of Molecular Biology 76:45-60.
589 49. Aksyuk AA, Rossmann MG. 2011. Bacteriophage assembly. Viruses 3:172-203.
590 50. Cobbold C, Windsor M, Wileman T. 2001. A virally encoded chaperone specialized for folding
591 of the major capsid protein of African swine fever virus. Journal of virology 75:7221-7229.
592 51. Spence SL, Pipas JM. 1994. SV40 Large T Antigen Functions at Two Distinct Steps in Virion
593 Assembly. Virology 204:200-209.
594 52. Suzuki H. 1996. A hypothesis about the mechanism of assembly of double-shelled rotavirus
595 particles, p 79-85, Viral Gastroenteritis. Springer.
596 53. Vance LM, Moscufo N, Chow M, Heinz BA. 1997. Poliovirus 2C region functions during
597 encapsidation of viral RNA. Journal of virology 71:8759-8765.
598 54. Asare E, Mugavero J, Jiang P, Wimmer E, Paul AV. 2016. A Single Amino Acid Substitution in
599 Poliovirus Nonstructural Protein 2CATPase Causes Conditional Defects in Encapsidation and
600 Uncoating. Journal of virology 90:6174-6186.
601 55. Liu Y, Wang C, Mueller S, Paul AV, Wimmer E, Jiang P. 2010. Direct interaction between two
602 viral proteins, the nonstructural protein 2C and the capsid protein VP3, is required for
603 enterovirus morphogenesis. PLoS pathogens 6:e1001066-e1001066.
604 56. Hellen CU, Lee CK, Wimmer E. 1992. Determinants of substrate recognition by poliovirus 2A
605 proteinase. Journal of virology 66:3330-3338.
606 57. Dulbecco R, Vogt M. 1954. Plaque formation and isolation of pure lines with poliomyelitis
607 viruses. J Exp Med 99:167-82.
608 58. Chomczynski P, Sacchi N. 2006. The single-step method of RNA isolation by acid guanidinium
609 thiocyanate-phenol-chloroform extraction: twenty-something years on. Nat Protoc 1:581-5.
610 59. Kitamura N, Wimmer E. 1980. Sequence Studies of Poliovirus Rna .5. Sequence of 1060-3'-
611 Terminal Nucleotides of Poliovirus Rna as Determined by a Modification of the
612 Dideoxynucleotide Method. Proceedings of the National Academy of Sciences of the United
613 States of America-Biological Sciences 77:3196-3200.
614 60. Chen S, Songkumarn P, Liu J, Wang GL. 2009. A versatile zero background T-vector system
615 for gene cloning and functional genomics. Plant Physiol 150:1111-21.

616 61. Cornell CT, Perera R, Brunner JE, Semler BL. 2004. Strand-specific RNA synthesis
617 determinants in the RNA-dependent RNA polymerase of poliovirus. J Virol 78:4397-407.
618 62. Semler BL, Johnson VH, Dewalt PG, Ypmawong MF. 1987. Site-Specific Mutagenesis of Cdna
619 Clones Expressing a Poliovirus Proteinase. Journal of Cellular Biochemistry 33:39-51.
620 63. Studier FW, Moffatt BA. 1986. Use of bacteriophage T7 RNA polymerase to direct selective
621 high-level expression of cloned genes. Journal of Molecular Biology 189:113-130.
622 64. Herod MR, Ferrer-Orta C, Loundras EA, Ward JC, Verdaguer N, Rowlands DJ, Stonehouse NJ.
623 2016. Both cis and trans Activities of Foot-and-Mouth Disease Virus 3D Polymerase Are
624 Essential for Viral RNA Replication. J Virol 90:6864-6883.
625 65. Weber K, Osborn M. 2006. SDS-PAGE to determine the molecular weight of proteins: The
626 work of Klaus Weber and Mary Osborn - The reliability of molecular weight determinations
627 by dodecyl sulfate-polyacrylamide gel electrophoresis (reprinted from J.Biol. Chem. vol. 244,
628 pg. 4406-4412, 1969). Journal of Biological Chemistry 281.
629 66. Circolo A, Gulati S. 2009. Autoradiography and Fluorography of Acrylamide Gels. Protein
630 Protocols Handbook, Third Edition doi:Doi 10.1007/978-1-59745-198-7_56:595-603.
631 67. Johnston RF, Pickett SC, Barker DL. 1990. Autoradiography using storage phosphor
632 technology. Electrophoresis 11:355-60.
633 68. Brown BA, Ehrenfeld E. 1979. Translation of poliovirus RNA in vitro: changes in cleavage
634 pattern and initiation sites by ribosomal salt wash. Virology 97:396-405.
635 69. Mahmood T, Yang P-C. 2012. Western Blot: Technique, Theory, and Trouble Shooting. North
636 American Journal of Medical Sciences 4:429-434.
637 70. Schneider CA, Rasband WS, Eliceiri KW. 2012. NIH Image to ImageJ: 25 years of image
638 analysis. Nat Methods 9:671-5.
639

640 **Figure 1. Identification of thermally selected mutations.** *(A) Cartoon structure of PV*
641 *genome. Figure shows the 5' and 3' UTRs flanking the open reading frame comprising the*
642 *structural (P1) and non-structural (P2, P3) regions. (B) Evolution of PV-1 under thermal*
643 *selection. Viral RNA was extracted from each passage of virions selected at 51°C (i.e. VS51),*
644 *53°C (i.e. VS53) and 57°C (i.e. VS57) (25). The entire genome of the evolving population at*
645 *each passage was reverse-transcribed and amplified by PCR. The virus pool was sequenced*
646 *and aligned against the wt PV-1 sequence by ClustalOmega. Figure shows cartoon*
647 *representation of selected mutations. Solid black vertical lines represent wt sequences of the*
648 *P1 and 2A regions. Non-synonymous mutations are presented as coloured shapes in VP4 (●),*
649 *VP2 (◆), VP3 (▲), VP1 (■) and 2A^{pro} (★) as shown in the key insert. (C) Sequence*
650 *comparisons of 2A^{pro} among enteroviruses. Alignment of 2A^{pro} amino acid sequences of*
651 *thermally selected viruses VS51, VS53 and VS57 against enterovirus A: Coxsackievirus A1*
652 *(CVA-1); enterovirus B: echovirus 1 (EV1); enterovirus C: PV-1, PV-2, PV-3 and CVA-2;*
653 *enterovirus D: human enterovirus 94 (EV-94); enterovirus E: bovine enterovirus (BEV-1);*
654 *enterovirus F: BEV-2; enterovirus G: porcine enterovirus G1 (EV-G1); enterovirus H:*
655 *simian enterovirus SV4 (SV4); rhinovirus A: human rhinovirus A (HRVA); rhinovirus B:*
656 *HRV-B and rhinovirus C: HRV-C. Figure shows the alignment of a 60-residue region of*
657 *2A^{pro}. Thermally selected virions are underlined as VS51, VS53 and VS57. Enterovirus C*
658 *members are annotated with a bracket. The 2A^{pro} consensus residues of wt PV-1 are shown in*
659 *bold letters. Matching residues are shown as dots beneath corresponding residues of wt PV-*
660 *1. Variable residues are shown in capital letters underneath corresponding position of the wt*
661 *PV-1 residues. Asterisks on consensus sequence indicate positions that correspond to*
662 *residues I99 and G102, respectively. Sequences were aligned using default alignment*
663 *algorithms of CLC sequencing viewer version 6.*

664

665 **Figure 2. Effect of 2A^{pro} mutations on cis cleavage activity at P1/2A junction.** *(A)*
666 *Cartoon of the construct used in the transcription/translation T_NT assay. (B)*
667 *Autoradiographs of SDS-PAGE of T_NT samples. Following incubation at 30°C for 90*
668 *minutes, further incorporation of ^{35}S (cys/met) was prevented by the addition of excess*
669 *unlabelled cys/met and samples collected at 30-minute intervals. Samples were separated by*
670 *SDS-PAGE and protein bands detected by autoradiography. Arrows correspond to P1/2Apro*
671 *precursor and processed P1. Time points represent chase. Normalised densitometry of*
672 *P1/2Apro precursor (C) and cleaved P1 (D) over time. Graphs represents intensity of P1*
673 *band of phosphoscreen scans of autoradiograph. Scanned images were analysed by ImageJ*
674 *version 1.47t. (n = 2 ± S.E.M., **P<0.001 compared to wt).*

675

676 **Figure 3. Polyprotein processing of wt and 2A^{pro} mutant PV-1.** *(A) Both 2A mutations*
677 *were introduced into an infectious clone of wt PV-1 (i.e. pt7Rbz). RNA-transcripts of pt7Rbz*
678 *or 2A-I99V/-G102R were used in HeLa cell-free reactions. Following incubation at 34˚C for*
679 *2 hours, excess cys/met was added and samples taken at various time points. Samples (lanes*
680 *1 – 12) were separated by 8% SDS-PAGE and radio-labelled proteins detected by*
681 *autoradiography. To identify specific bands, pcDNA constructs of P1, P2, non-cleavable P1-*
682 *2A and non-cleavable P1-P2 were expressed in T_NT reactions in the presence of ^{35}S [cys/met]*
683 *and incubated for 3 hours (lanes 13 – 17). Band intensities were quantified from a*
684 *phosphoscreen image and the levels of (B) P1-P2 and (C) P1-2A presented as normalised*
685 *percentage (%) intensity over background phosphorescence. Scanned images were analysed*
686 *by ImageJ version 1.47t (n = 3 ± S.E.M., *P<0.05, **P<0.001 compared to wt at each time*
687 *point).*

688

689 **Figure 4. Effect of 2A^{pro} mutations on PV-1 replicon replication.** *(A) HeLa cells were*

690 *transfected with T7 RNA transcripts and replication monitored by GFP fluorescence over*

691 *time using an IncuCyte ZOOM. A replication-deficient mutant, 3D-GNN, was included as*

692 *control for input translation. (B) The data from (A) at 22 hours post-transfection (total GFP*

693 *positive cells) were also plotted as a bar graph for clarity (n = 3 ± S.E.M., *P<0.05,*

694 ***P<0.001, ***P<0.0001).*

695 **Figure 5. Effects of 2A^{pro} mutations on virus recovery.** *RNA-transcripts were generated*
696 *from infectious clones of wt or VP1-I194V in the presence or absence of the 2A^{pro} mutations*
697 *2A-I99V/-G102R, transfected into HeLa cells and incubated at 37°C for 24 hours. (A) Virus*
698 *titres recovered from transfected mouse L-cells (n = 3 ± S.E.M., ***P<0.0001) (B) Virus*
699 *titres recovered from transfected HeLa cells. (n = 3 ± S.E.M., ***P<0.0001) (C) Virus*
700 *samples recovered from HeLa cells were diluted in serum-free media to equal starting titres*
701 *and incubated at a range of temperatures between 37°C and 55°C for 30 minutes, cooled to*
702 *4°C and titrated by plaque assays using HeLa cells (n = 2 ± S.D. *P<0.05 compared to wt).*
703

704 **Figure 6. Effects of reduced translation on assembly-deficient VP1-I194V mutant.** *(A)*
705 *Mouse L-cells were treated with increasing concentrations of cycloheximide and assayed for*
706 *toxicity by MTS.* IC_{50} *was evaluated by dose-dependent curves (n = 2 ± S.D.) (B) Mouse L-*
707 *cells were transfected with T7 RNA transcripts of wt and treated with cycloheximide at*
708 *increasing concentrations. Cell lysates were harvested using RIPA buffer. Supernatants and*
709 *cell lysates were separated respectively by SDS-PAGE and immunoblotted against anti-PV-1*
710 *VP1 MAb 8560. Figure shows representative of two biological repeats. (C) Mouse L-cells*
711 *were transfected with T7 RNA transcripts of wt and VP1-I194V mutant and treated at two*
712 *concentrations of cycloheximide. Supernatant were clarified by low speed centrifugation.*
713 *Virus titres of supernatants from cycloheximide-treated wt and VP1-I194V mutant-*
714 *transfected cells were determined by plaque assays using HeLa cells (n = 2 ± S.E.M.,*
715 **P<0.05, ***P<0.0001 compared to non-treated wt).*

716

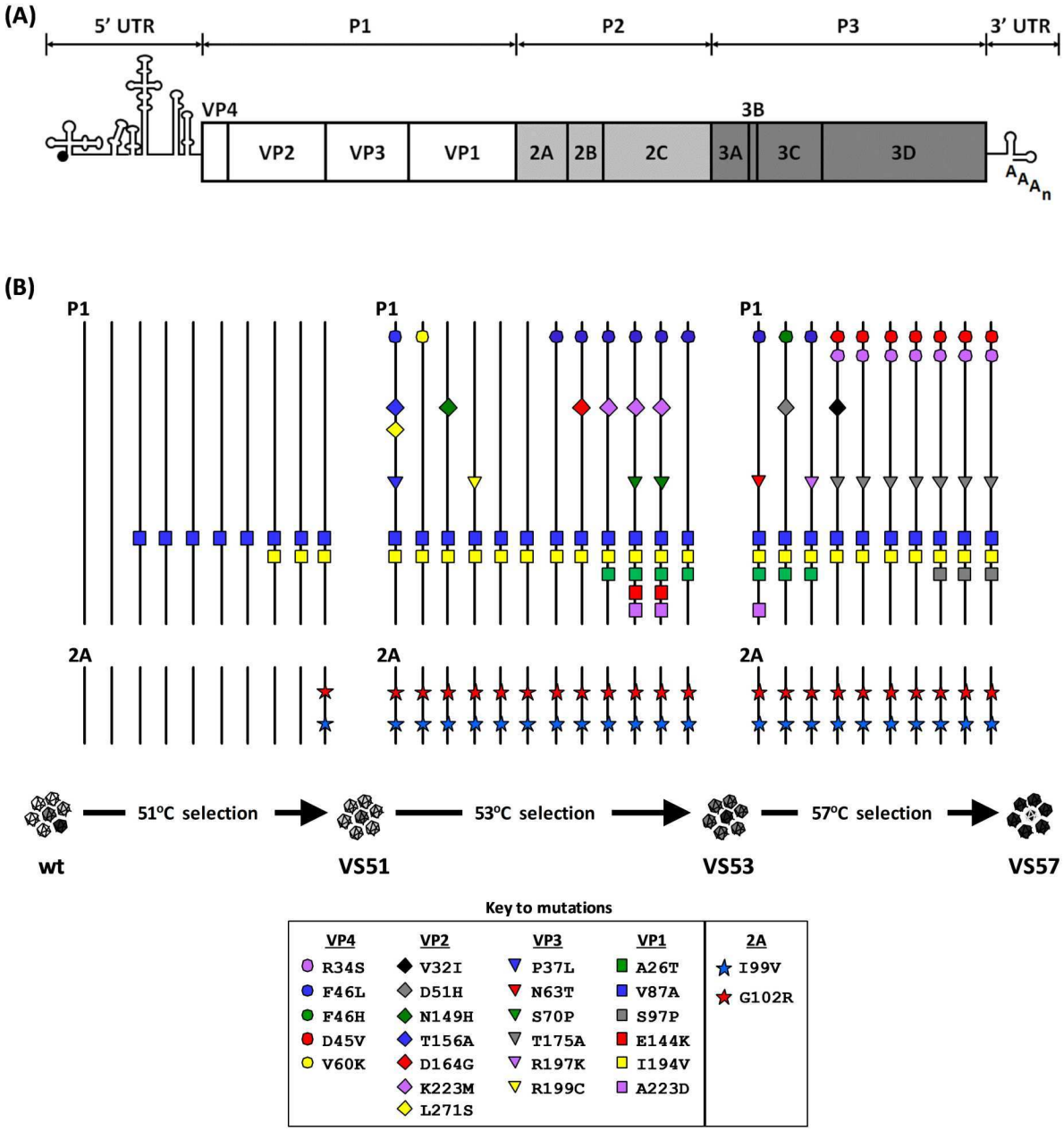

(C)

```
                                                                  *    *
Enterovirus C
PV-1    GVYYCESRRK YYPVSFVGPT FQYMEANNYY PARYQSHMLI GHGFASPGDC GGILRCHHGV 119
VS51    .......... .......... .......... .........V ..R....... .......... 119
VS53    .......... .......... .......... .........V ..R....... .......... 119
VS57    .......... .......... .......... .........V ..R....... .......... 119
PV-2    .......... ......T... .......E.. .......... .......... ......Q... 119
PV-3    .......... .......... .......D.. .......... .......... ......Q... 119
CVA-1   .I......K.. ...I.VC... .......DF. .......... .Y...N.... ......Q... 119
CVA-2   .....N.... H.....SK.S LVFV..SE.. .......LML AV.HSE.... ......Q... 120
EV1     ...F.L..N. H.....E..G LVEVQESE.. .K.....V.L AA..SE.... ......E... 120
EV-G1   ...F.K..N. H...T.Q..G IDWV..SR.. .....T.... AA.ISE.... ..V..-Q... 119
BEV-1   .I...K.TA. H..IVVTP.S IYKI...D.. .E.M.T.I.L .I...E.... ..L...E... 120
BEV-2   .....K..G. H...VVTP.S LVHVD..D.. .E.....V.L .I...E.... ......Q..C 120
EV-94   .....RH.DR S...C.E..G I.WV.E.E.. .....TNT.L AN.PVEA... ..L.V.P... 117
SV4     ...WSRTYG. CF.AY.Q..G IEKFQ.SE.. .E...T.V.L AM.P.Q.... ..L.C.P... 117
HRV-B26 ....SRYYN. F..IVCEK.. CLWI.G.... .S...QGVMR .V.P.E.... .....I..P 119
HRV-A2  AT...KHKNR .F.ITVTSHD WYEIQESE.. .KHI.YNL.. .E.PCE.... ..K.L.K... 116
HRV-C   .T.F.K.MDR ....E.RHHS WYEIQESI.. .KHI.YDI.. .E.PC..... ..K.L.V..T 115
```

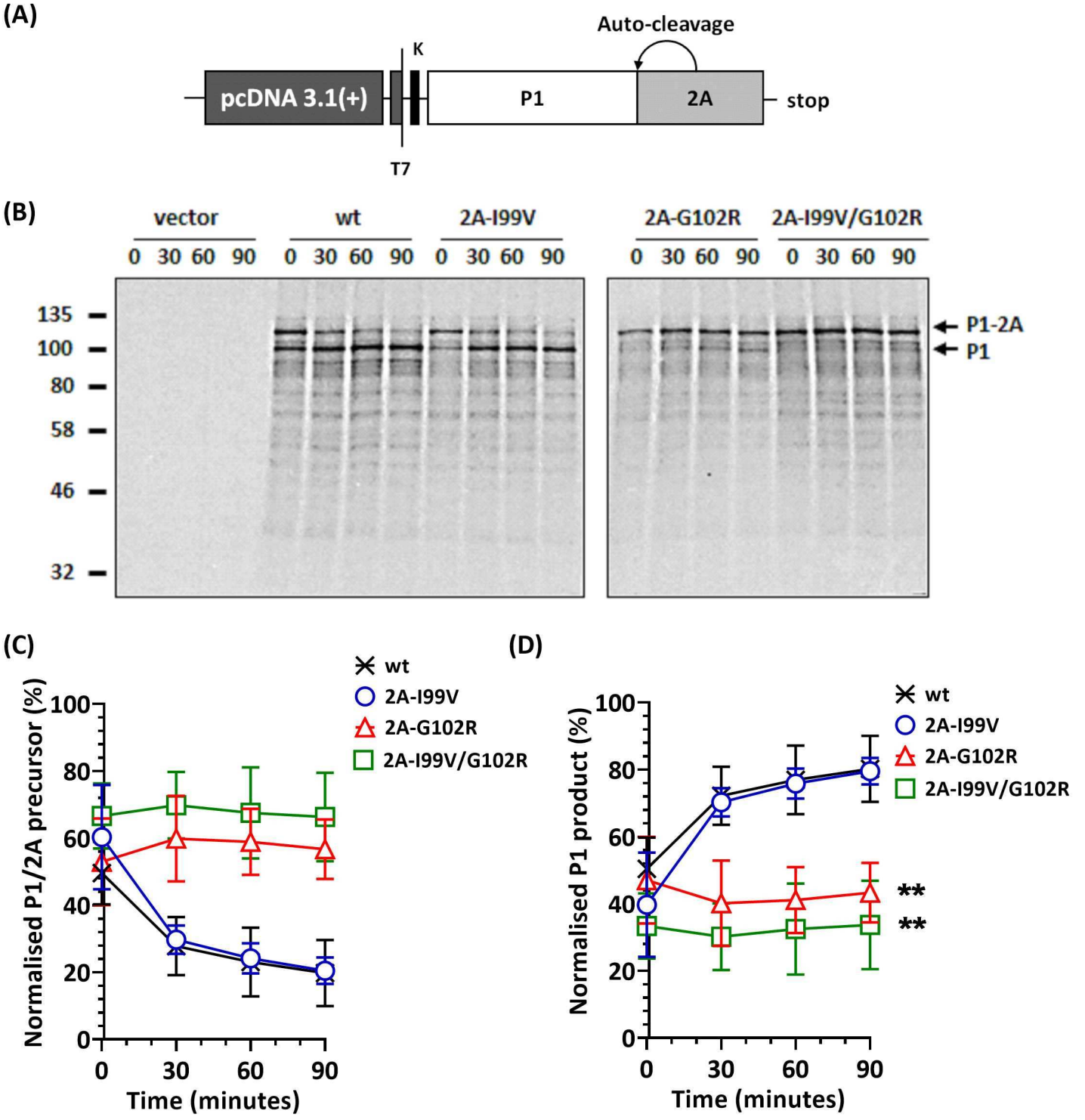
(A)
Auto-cleavage
K
pcDNA 3.1(+)
P1
2A
stop
T7
(B)
vector
wt
2A-I99V
2A-G102R
2A-I99V/G102R
0 30 60 90
135
100
80
58
46
32
P1-2A
P1
(C)
wt
2A-I99V
2A-G102R
2A-I99V/G102R
Normalised P1/2A precursor (%)
Time (minutes)
(D)
Normalised P1 product (%)
**
**
Time (minutes)

(A)

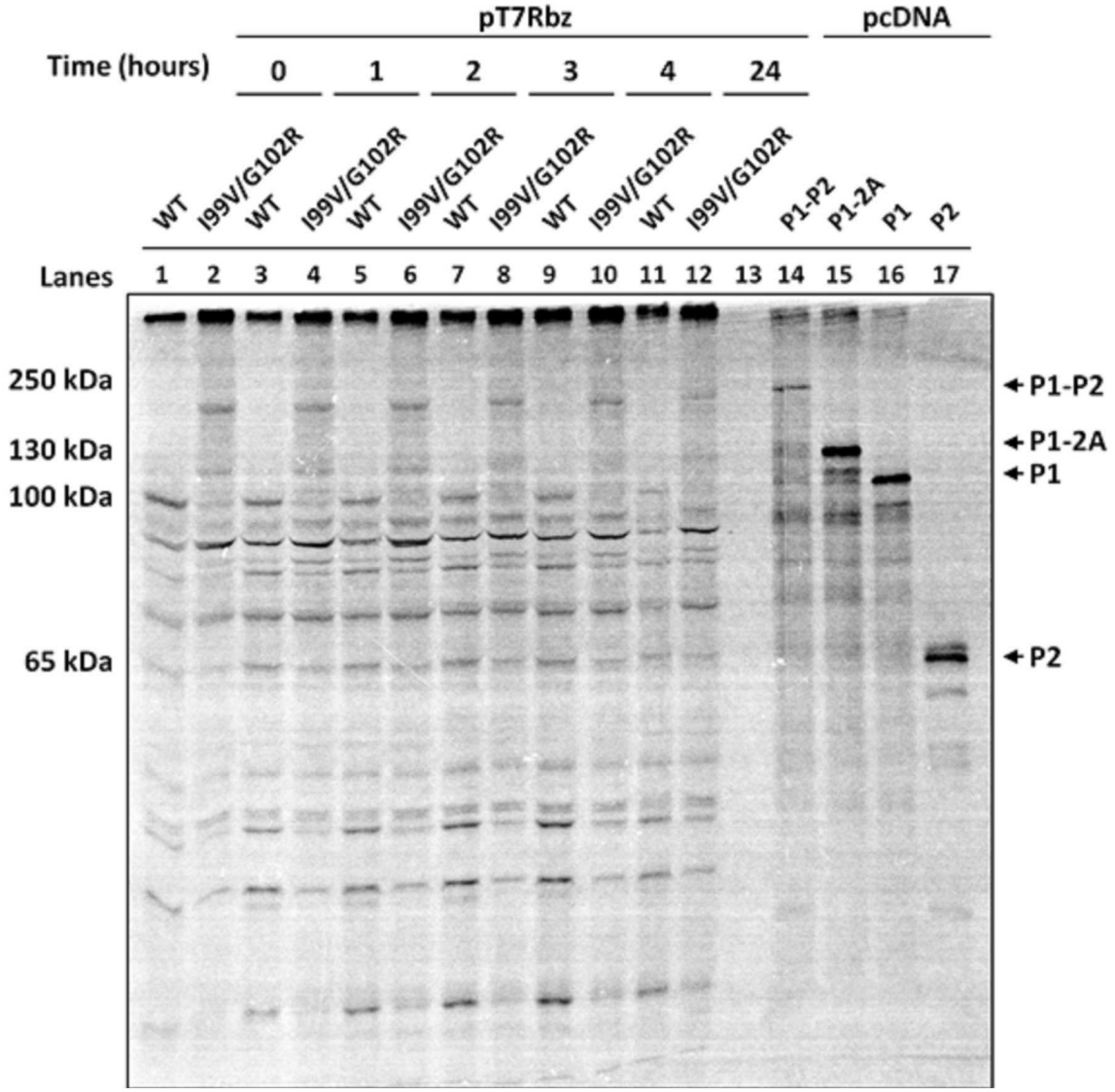
pT7Rbz
pcDNA
Time (hours)
0
1
2
3
4
24
WT
I99V/G102R
P1-P2
P1-2A
P1
P2
Lanes
1 2 3 4 5 6 7 8 9 10 11 12 13 14 15 16 17
250 kDa
130 kDa
100 kDa
65 kDa
P1-P2
P1-2A
P1
P2

(B)

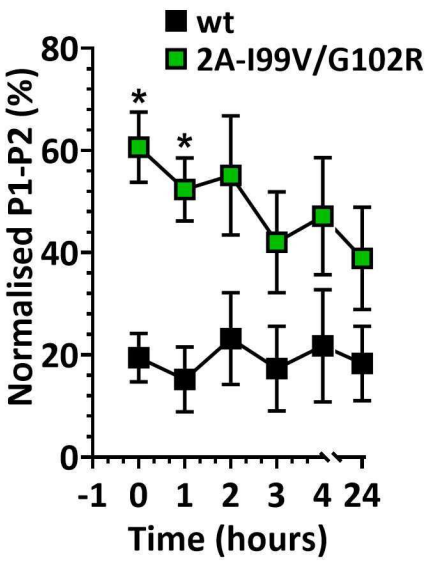
wt
2A-I99V/G102R
Normalised P1-P2 (%)
0
20
40
60
80
-1 0 1 2 3 4 24
Time (hours)

(C)

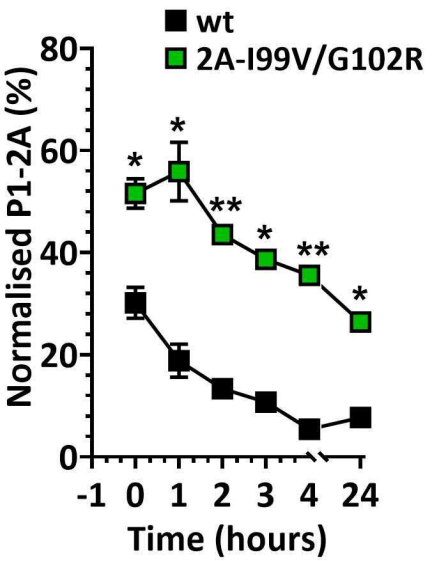
wt
2A-I99V/G102R
Normalised P1-2A (%)
0
20
40
60
80
-1 0 1 2 3 4 24
Time (hours)

(A)

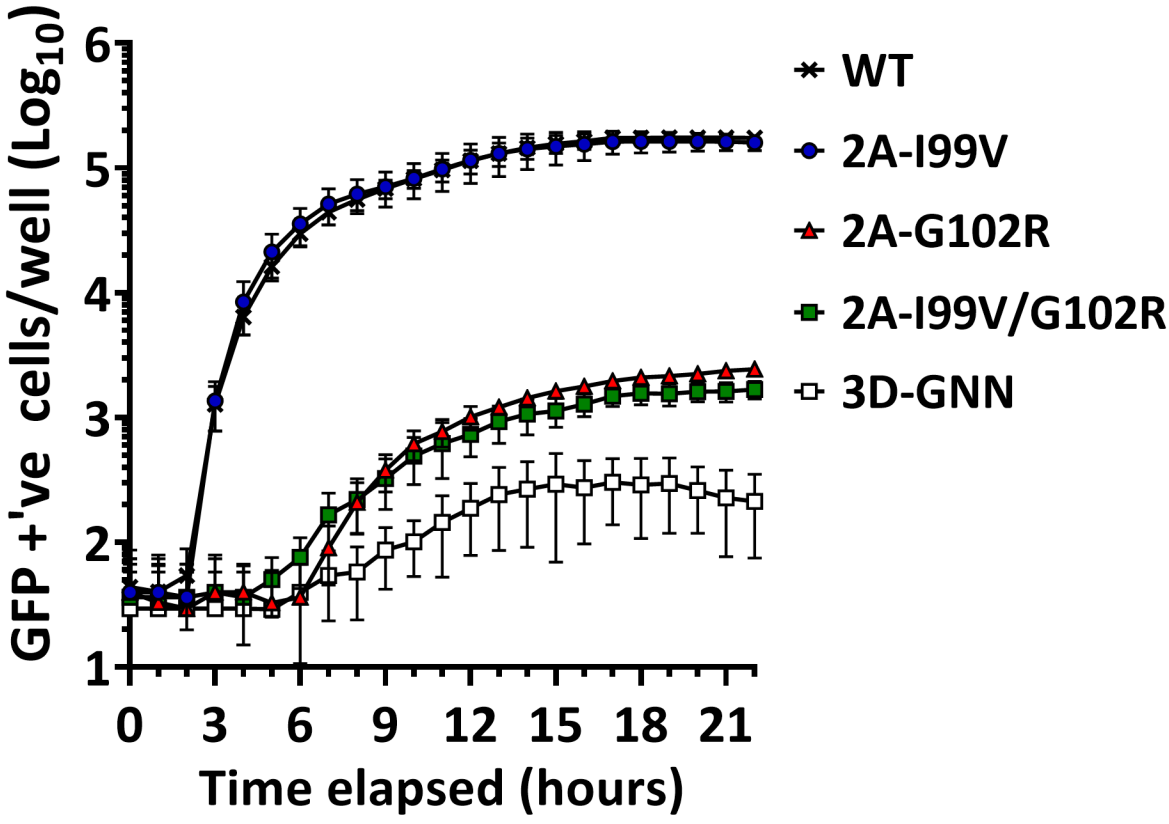
GFP +'ve cells/well (Log10)
6
5
4
3
2
1
0
3
6
9
12
15
18
21
Time elapsed (hours)
WT
2A-I99V
2A-G102R
2A-I99V/G102R
3D-GNN

(B)

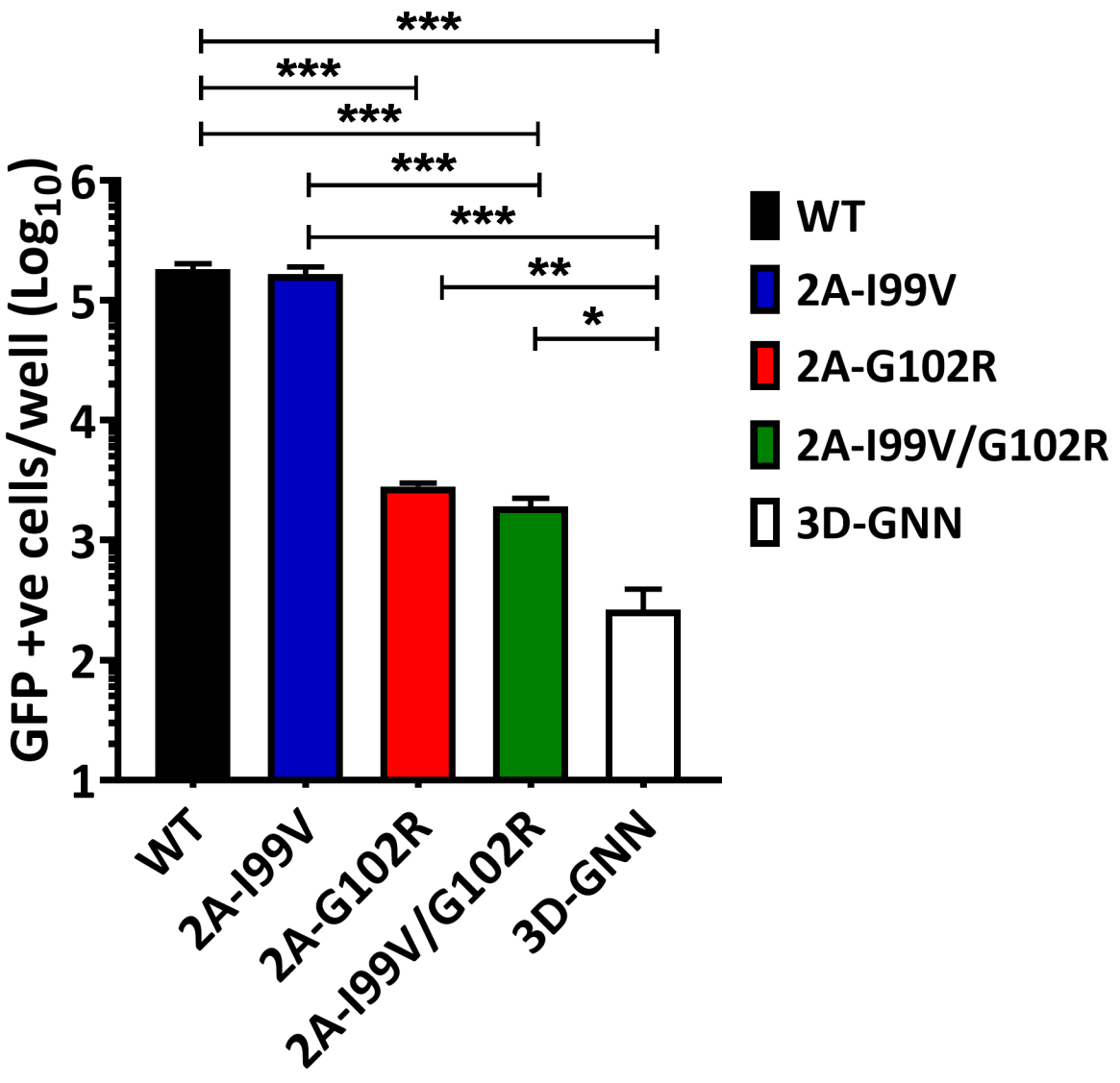
GFP +ve cells/well (Log10)
6
5
4
3
2
1
***
***
***
***
***
**
*
WT
2A-I99V
2A-G102R
2A-I99V/G102R
3D-GNN
WT
2A-I99V
2A-G102R
2A-I99V/G102R
3D-GNN

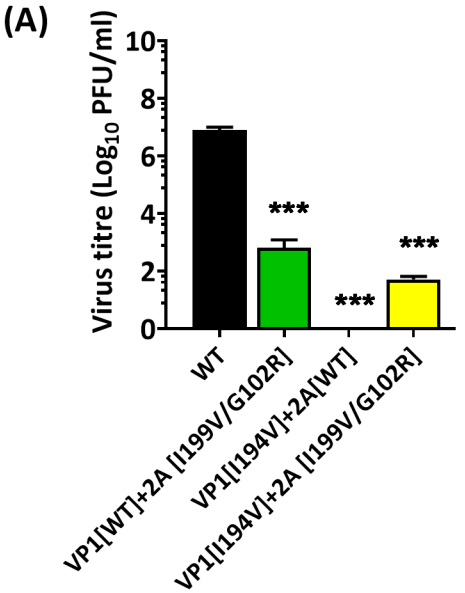
(A)
Virus titre (Log10 PFU/ml)
10
8
6
4
2
0
***
***
***
WT
VP1[WT]+2A [I199V/G102R]
VP1[I194V]+2A[WT]
VP1[I194V]+2A [I199V/G102R]

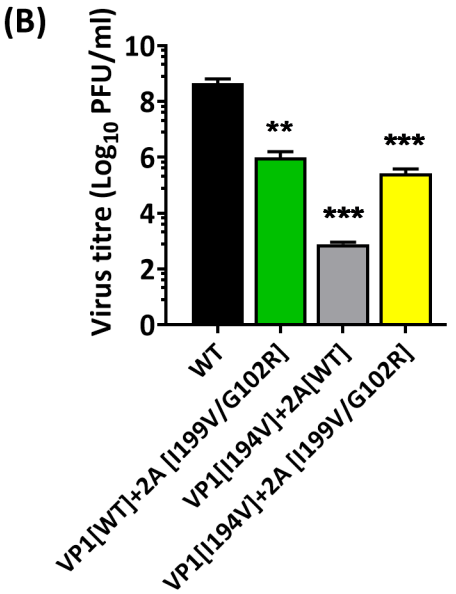
(B)
Virus titre (Log10 PFU/ml)
10
8
6
4
2
0
**
***
***
WT
VP1[WT]+2A [I199V/G102R]
VP1[I194V]+2A[WT]
VP1[I194V]+2A [I199V/G102R]

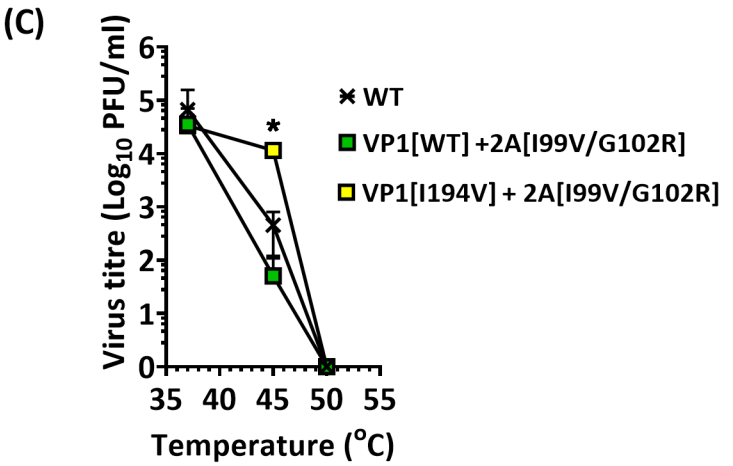
(C)
Virus titre (Log10 PFU/ml)
6
5
4
3
2
1
0
*
35
40
45
50
55
Temperature (°C)
WT
VP1[WT] +2A[I99V/G102R]
VP1[I194V] + 2A[I99V/G102R]

(A)

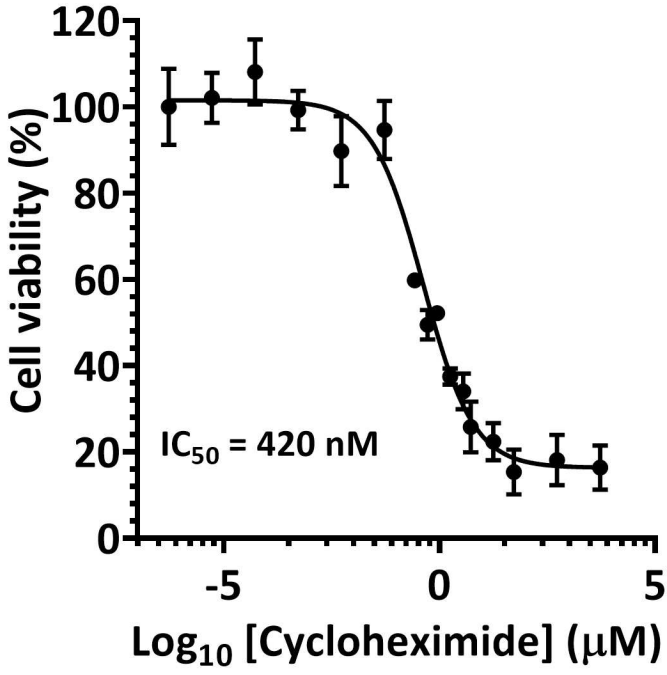
Cell viability (%)
120
100
80
60
40
20
0
IC50 = 420 nM
-5
0
5
Log10 [Cycloheximide] (μM)

(B)

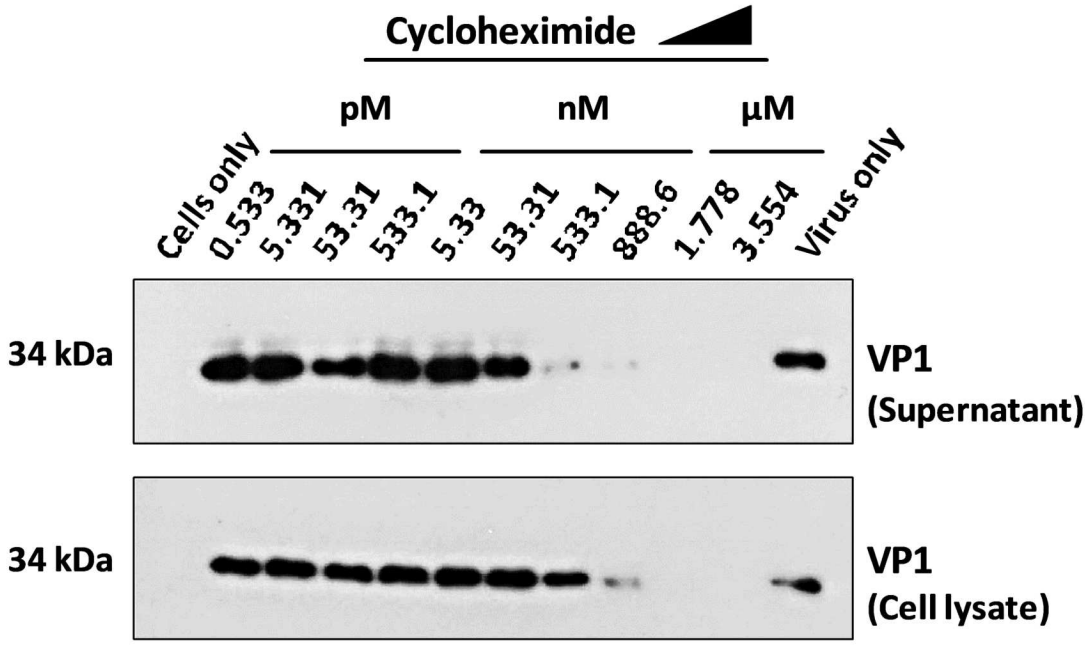
Cycloheximide
pM
nM
μM
Cells only
0.533
5.331
53.31
533.1
5.33
53.31
533.1
888.6
1.778
3.554
Virus only
34 kDa
VP1
(Supernatant)
34 kDa
VP1
(Cell lysate)

(C)

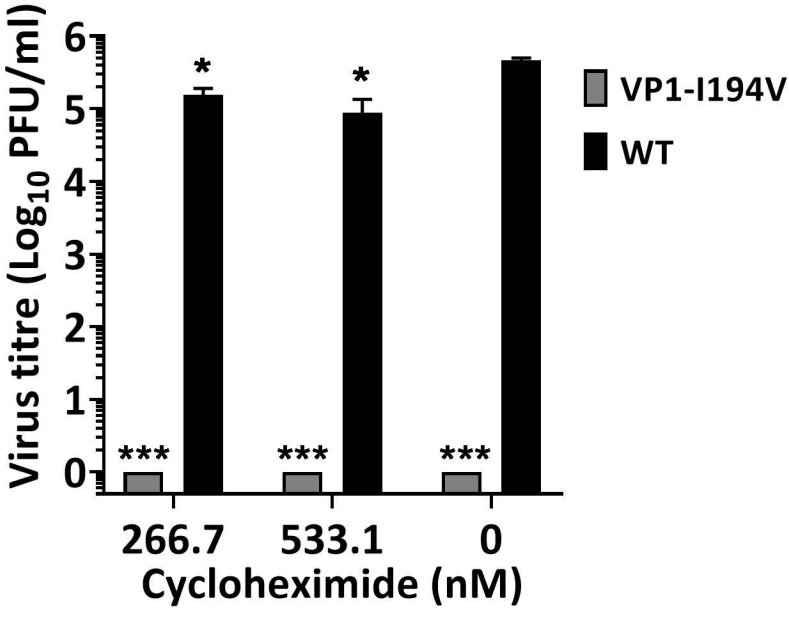
Virus titre (Log10 PFU/ml)
6
5
4
3
2
1
0
*
*
***
***
***
VP1-I194V
WT
266.7
533.1
0
Cycloheximide (nM)

Table 1. Recovery of infectious virions with mutations in structural proteins

Capsid mutation[(a)]	Mutant construct[(b)]	Recovery of infectious virion
VP1-A26T	pT7Rbz-PV1-VP1$_{A26T}$	Yes
VP1-V87A	pT7Rbz-PV1-VP1$_{V87A}$	Yes
VP1-S97P	pT7Rbz-PV1-VP1$_{S97P}$	Yes
VP1-I194V	pT7Rbz-PV1-VP1$_{I194V}$	No
VP3-C175A	pT7Rbz-PV1-VP3$_{C175A}$	Yes
VP4-R34S	pT7Rbz-PV1-VP4$_{R34S}$	Yes
VP4-D45V	pT7Rbz-PV1-VP4$_{D45V}$	Yes
VP4-F46L	pT7Rbz-PV1-VP4$_{F46L}$	Yes

(a) Structural mutations identified in previously reported thermally selected viruses (34)

(b) Capsid mutations were individually introduced into cDNA, pT7Rbz-PV1 by site-directed mutagenesis. T7 RNA transcripts were transfected into mouse L-cells and infectious virion recovered were titrated by plaque assays using HeLa cells (n=3).